March 1992

Energy & Technology Review

- Numerical Simulation in Realistic Geometries
- Kestrel: A High-Altitude Balloon Platform
- Increasing Laser Power with Beamlet Architecture

University of California
Lawrence Livermore National Laboratory

Increasing Laser Power With Beamlet Architecture

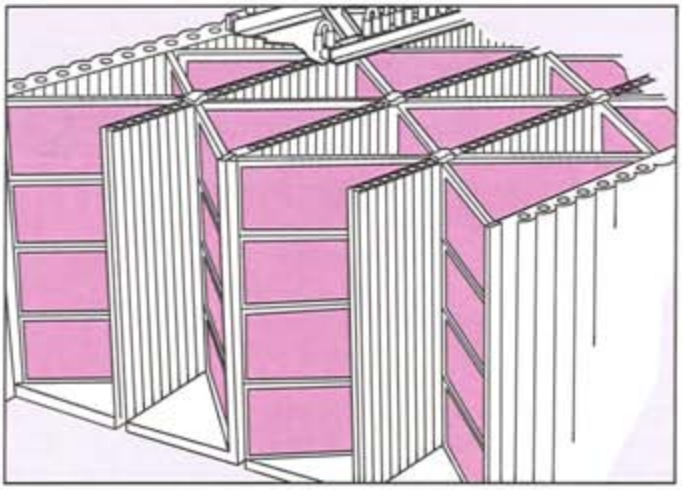

Our new modular laser architecture will provide the increased laser power needed for advanced inertial confinement fusion experiments.

HIGH-POWER lasers are used to produce very brief and extremely powerful pulses for inertial confinement fusion (ICF) experiments. The powerful pulses of energy rapidly heat and compress a small target sphere filled with thermonuclear fuel. If the target is heated and compressed with sufficient speed, nuclear fusion reactions will take place before the target disintegrates. Studies of ICF under laboratory conditions began at LLNL and elsewhere in the late 1960s. Since then, much has been learned about the complex physics of ICF targets and the energy pulses required to induce thermonuclear reactions in them.

Most laboratory studies of ICF use large lasers based on neodymium glass. The largest and most powerful of these systems is the Nova laser facility (Figure 1) now operating at LLNL.[1] The Nova laser can produce up to 120 kJ of light in a pulse that is a few nanoseconds in length at its fundamental wavelength of 1053 nm in the near-infrared. Typical fusion target experiments on Nova use 20–40 kJ of light in 1- to 2-ns pulses at the third harmonic of the laser, 351 nm, in the ultraviolet.

In September of 1990, the National Academy of Sciences Review Committee for the Inertial Fusion Program submitted its final report[2] to the Department of Energy. The report recommends that the next step in the ICF program be a facility to demonstrate the ignition of self-sustaining fusion. This step would be subject to successful completion of a number of target physics milestones and to a demonstration of the improved laser architecture and technology that we propose to use for the facility. The Department of Energy Fusion Policy Advisory Committee came to a similar conclusion.[3] In February of 1991, the Secretary of Energy sent a letter[4] to Congress that concurred with the recommendations of the National Academy Review Committee.

In response to these reports, we have established a Beamlet Demonstration Project to develop and demonstrate the improved technology and performance of the advanced glass laser needed for an ignition facility. In this context a "beamlet" is a single subaperture of the laser system that would contain perhaps 200 to 300 such beamlets in its final form. Each beamlet would

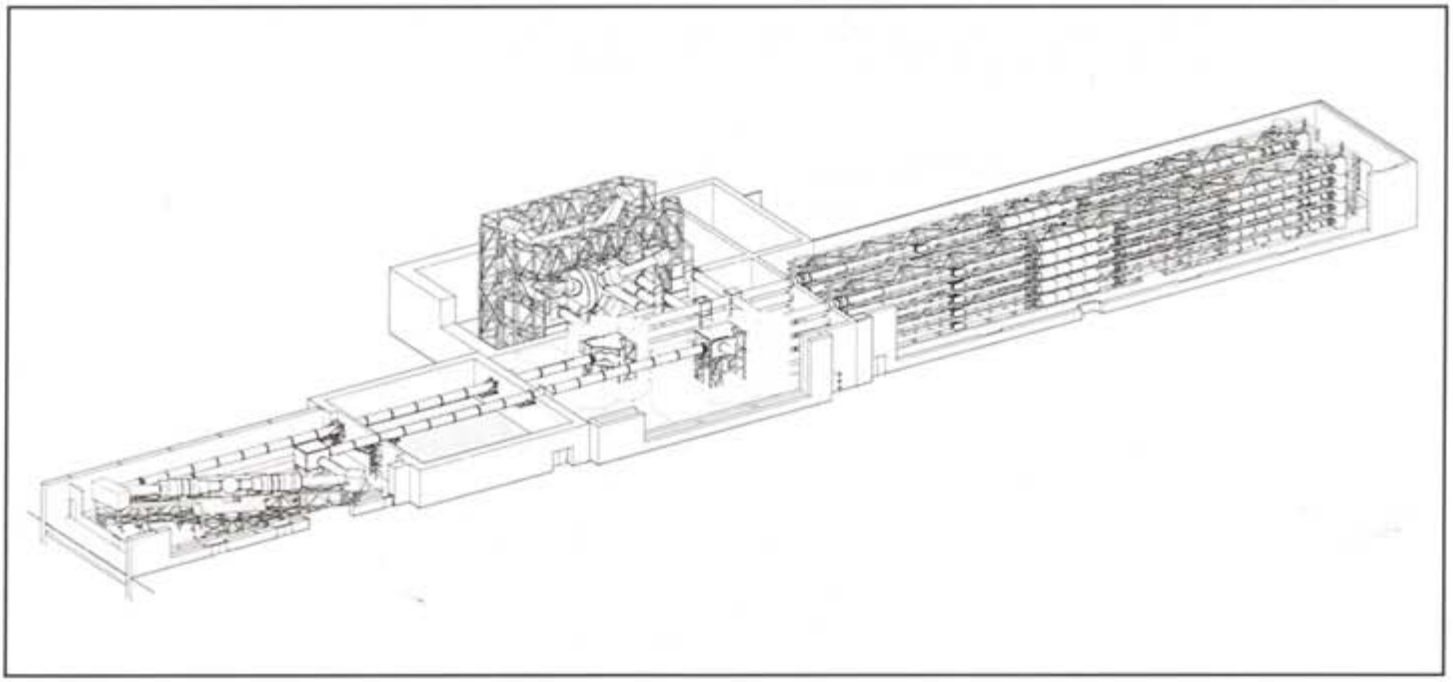

Figure 1. Present configuration of Nova, the world's most powerful laser and the newest in a series of increasingly powerful lasers developed at LLNL. Nova can produce a peak power output of 100 trillion watts. The output pulses can be shaped and tuned for maximum impact on fusion targets. Extensive recording and diagnostic capabilities provide a detailed record and analysis of experimental results.

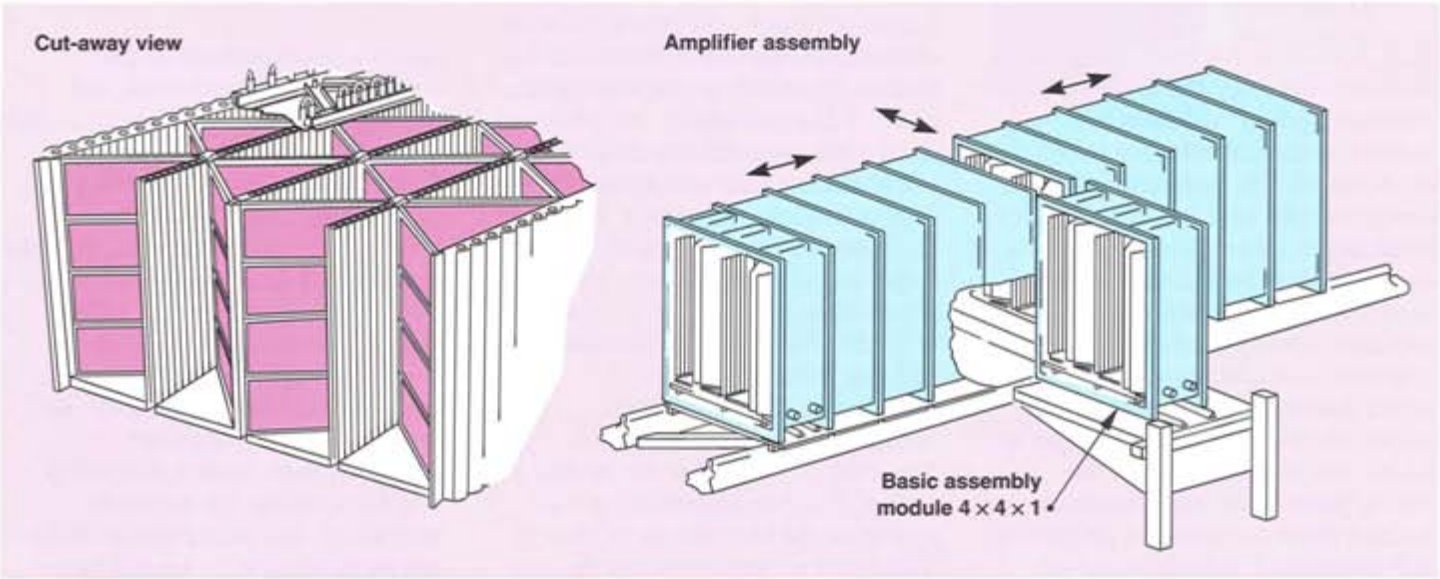

Figure 2. The multiple-segment amplifier. The glass slabs, reflectors, and flashlamps are assembled in modules. The amplifier will be built up from modules that are one slab deep and contain slabs arranged in a four-by-four array. Flashlamps running vertically between the slabs and along vertical walls will supply energy to the amplifier.

have an aperture of about 30 cm^2 and would deliver to the ignition target an output of 3.5 to 7.0 kJ (depending on the precise pulse shape) at 351 nm. We have chosen a 3-ns-long square output pulse as a nominal reference design point for simple discussions of beamlet performance since such a pulse is similar to the main, high-energy drive pulses required for present ignition target designs. In practice, a number of beamlets will be grouped together into a beamline based on an amplifier array, such as that shown in Figure 2.

The Beamlet will be constructed in the high-bay laboratory of Building 381, which was previously the site of the Argus and Novette ICF laser systems. Given present funding projections, we are planning to have the beamlet hardware demonstrate an initial performance milestone of 5 kJ at 350 nm in a 3-ns square pulse before the end of 1993.

This article gives an overview of the architecture that we propose to use for the Beamlet. Our emphasis is on the final amplifier stage, the high-energy beam transport stage, and the frequency-conversion stage since most of the cost and technical challenges of the system are in these large, high-fluence components.

Overview of the Laser Architecture

The final amplifier stage of the Beamlet will use slabs of neodymium-doped phosphate glass set at Brewster's angle to the beam (the angle at which the reflection from the glass surface goes to zero for a polarized beam) and pumped by xenon flashlamps. This is similar to the final amplifier stages of Nova and other large glass laser facilities. What is different is that the laser pulse makes several passes through a large-aperture final amplifier before exiting the laser and continuing on to the frequency converter and target chamber. Multipass amplifiers do not require as much input energy as single-pass amplifiers, which thus reduces the number of amplification stages and the cost of a facility. However, multipass systems do require a technique for separating the final output from earlier passes in the laser cavity. In the past, this requirement has restricted multipass lasers to rather small sizes.

The Beamlet facility will use a newly developed large-aperture optical switch, or Pockels cell, to extract the beam outlet. The Pockels cell consists of a thin plate of the electro-optic crystal KDP (potassium, dihydrogen, phosphate), or its deuterated analog KD*P, which rotates the polarization plane of the light passing through it when a voltage is applied parallel to the optical axis. A glow discharge in a low-pressure gas is used as a high-damage-threshold, transparent conducting electrode on the face of the crystal. The output beam is then extracted using a multilayer thin-film polarizer.

Damage to optical components sets limits to the intensity and fluence of high-energy lasers. Because the laser system is segmented into beamlets of fixed area, the cost of the laser hardware is roughly proportional to the total beam area. Thus, we must run the highest feasible fluence in the beam to minimize the area and cost. Since damage occurs in the regions of peak fluence, we can have higher average fluence, and hence higher output from each beamlet, if the output beam has a very uniform intensity profile with little intensity modulation.

Nova uses a technique called image relaying to improve beam uniformity and to reduce the growth of intensity ripples caused by diffraction.[5] We will also use this technique in the Beamlet facility. An image relay requires that we place two lenses with a common focal point between any two amplifiers (or between passes through a single amplifier) so that the image of the first amplifier lies on the second. Because the focal plane between the two lenses is also the Fourier-transform plane of the intensity profile of the beam, we can place a small aperture or "spatial filter pinhole" in that plane to remove high-spatial-frequency modulations from the beam. The nonlinear index of refraction of the optical components causes these high-spatial-frequency modulations, which have a spatial period of a few millimeters in the near-field, to grow rapidly in high-intensity pulses. By resetting the modulation to zero at several points in the laser chain, we can ensure that it never reaches a large amplitude.

Figure 3 shows a schematic diagram of the image-relayed, multipass final amplifier stage that we propose to use for the Beamlet facility demonstration. The laser pulse enters the cavity near the focal plane of an intracavity relay lens pair, L1 L2. It passes through an inner amplifier, A1, and reflects from mirror M1. It then passes through amplifier A2, the Pockels cell, and polarizer to reflect from mirror M2; passes through amplifiers A2 and A1 again; and reflects from mirror M1. At this point, the Pockels cell is fired to rotate the polarization so that the pulse reflects from the polarizer after its second roundtrip through the amplifier cavity and makes a single pass through the booster amplifier A3. The pulse then goes through an output image relay to a frequency

converter and on to the target chamber or laser diagnostics.

Mirrors M1 and M2 are positioned so that each pass of the beam is separated in the focal plane of the intracavity spatial filter and goes through a different pinhole, as shown in Figure 4. This configuration has several advantages. The separation allows us to install a small injection mirror near the focal plane and to inject the laser pulse conveniently at a small aperture. When a laser pulse goes through a pinhole, it generates a plasma from the edges of the pinhole. This plasma expands to fill the hole and may interfere with subsequent passes. Separate pinholes avoid this problem. The optical path in the cavity is not closed but terminates in the beam trap and injection path, which reduces the potential gain path length for the buildup of parasitic oscillations. If the switch leaks a small amount of energy on early passes, that energy propagates at a small angle to the final output pulse; thus, it does not go through the pinhole of the output image relay and cannot disturb the target. Also, if the switch fails to divert the energy from the cavity, the beam trap intercepts the output beam and prevents it from recirculating through the cavity and damaging optical components.

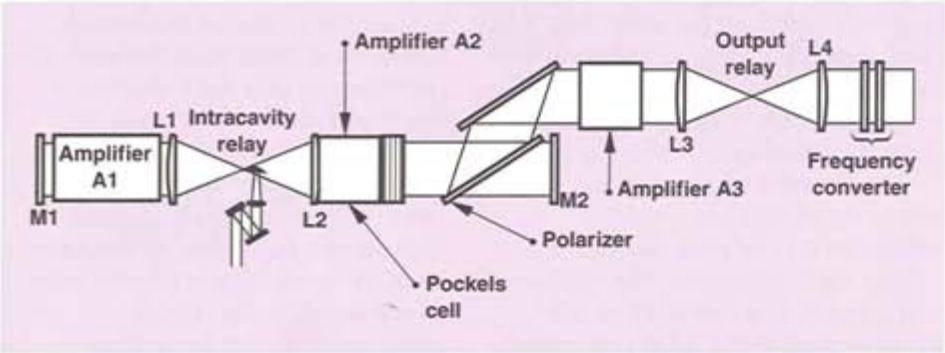

Figure 3. Laser configuration for the first series of the Beamlet project laser experiments. Specialized technology and high-purity laser glass are necessary to avoid equipment damage caused by the extremely high peak energy levels. The first series of experiments will have an amplifier inside the multipass cavity and a single-pass booster amplifier after the Pockels cell and polarizer. The output from the multipass cavity will be reflected from the polarizer.

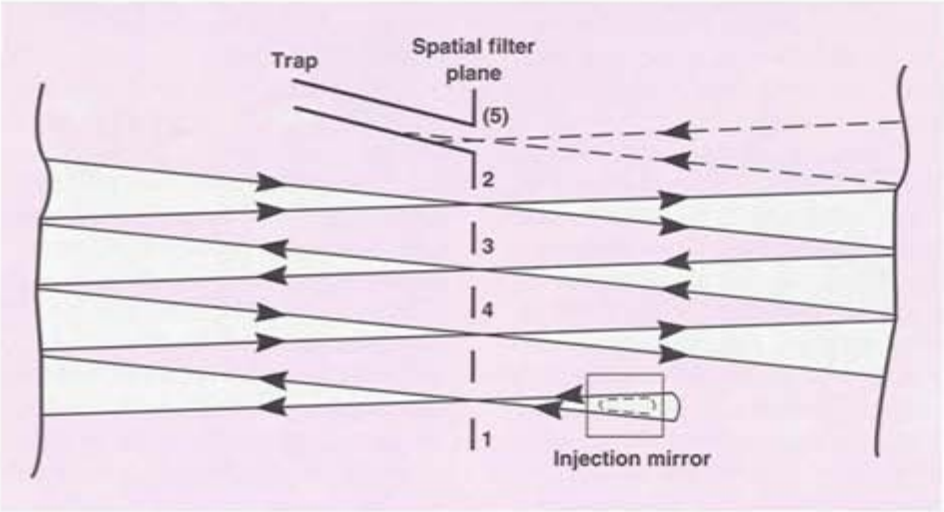

Figure 4. The intracavity relay focal plane, where beam filtering takes place. During each pass through the focal plane of the intracavity relay, the beam enters a separate pinhole. This permits convenient injection of energy into a small aperture and helps to mitigate a number of other problems, such as the buildup of high-frequency intensity modulations in the beam. At each pinhole, undesirable frequency components are removed by blocking selected portions of the beam's Fourier transform.

Because there are a number of minor design variations in a laser of this sort, we will design the hardware for the Beamlet to be flexible enough to explore these variations. For example, the output beam from the multipass might be extracted in transmission through the polarizer rather than in reflection.

Because a linear layout such as that shown in Figure 3 is a very tight fit in the space available in the high bay of Building 381, we will fold the Beamlet back on itself, using three mirrors between the polarizer and amplifier A3. Figure 5 is a drawing that shows how the Beamlet hardware will look after final assembly.

Amplifier Prototypes

We propose to build future ICF lasers from beamlines using a 16-beamlet amplifier array, as shown in Figure 2. A full beamline using this hardware would have nearly twice the output energy of the Nova laser and would be a

very expensive undertaking without the lower unit cost for mass procurement in a full-scale project. Since the beamlets are optically independent, a demonstration of laser performance on a single beamlet will adequately test the laser concept. This is the course we plan to follow.

We have constructed two amplifier prototypes (Figures 6 and 7) to explore the features of glass amplifiers with square rather than round apertures, and we could base the Beamlet demonstration on either one. One of these prototypes, the single-segment amplifier (SSA), has a single square aperture. The other, the multiple-segment amplifier (MSA), has four beamlets stacked in a two-by-two array and a mechanical

(a)

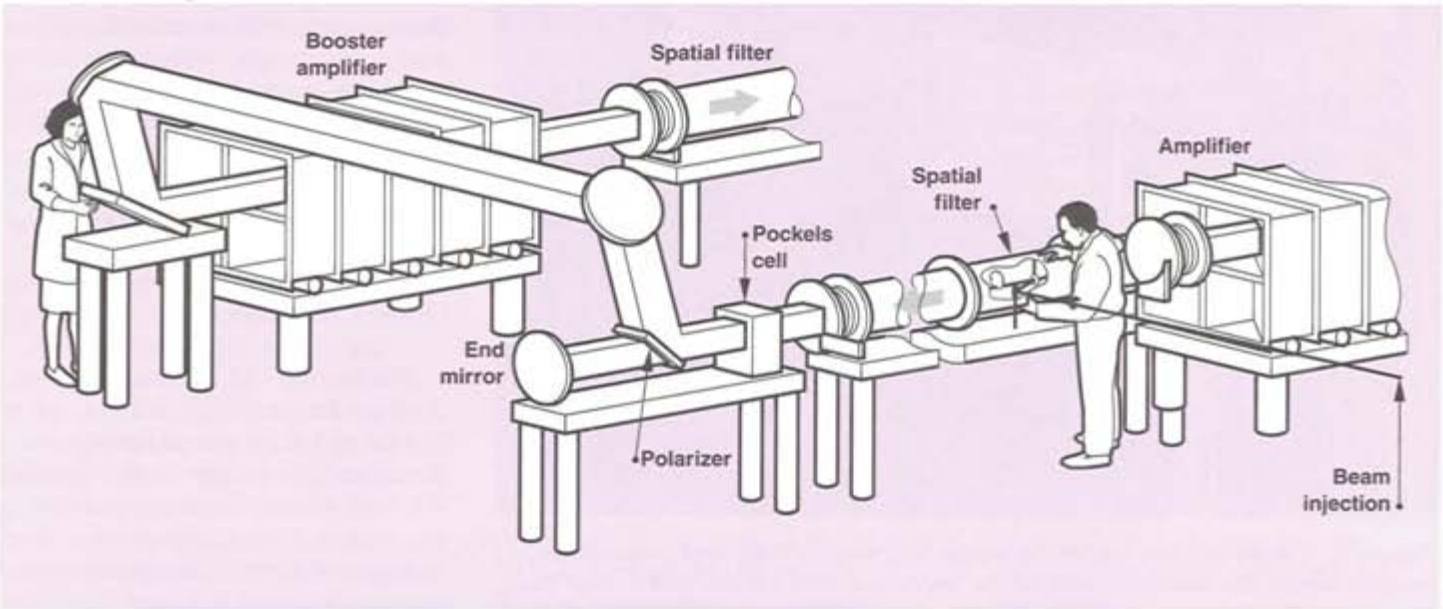

(b)

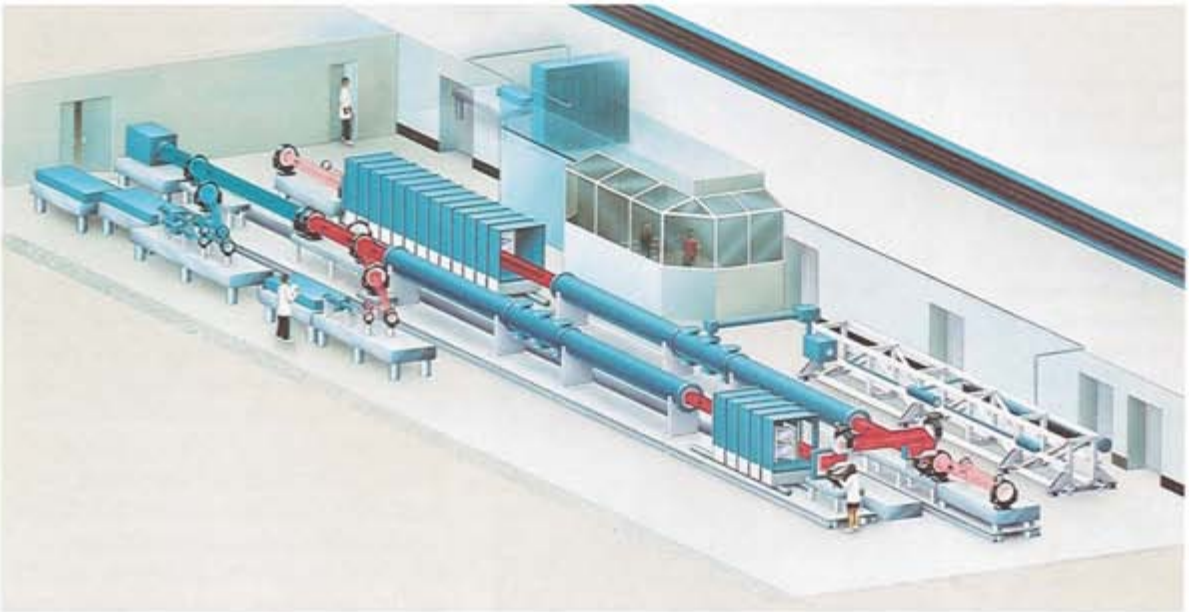

Figure 5. (a) A foreshortened schematic drawing of the folded Beamlet layout as it will appear in the high bay of Building 381. The entire optical train is filled with dry nitrogen to prevent contamination from particles in the air. (b) Artisit's rendering of the Beamlet in correct scale.

module unit that is one slab deep, similar to the four-by-four array shown in Figure 2. This prototype addresses the most important design difference between single-segment and multiple-segment amplifiers—flashlamps on an exterior wall with a reflector together with flashlamps in the center of an array to pump the amplifier slabs on both sides.

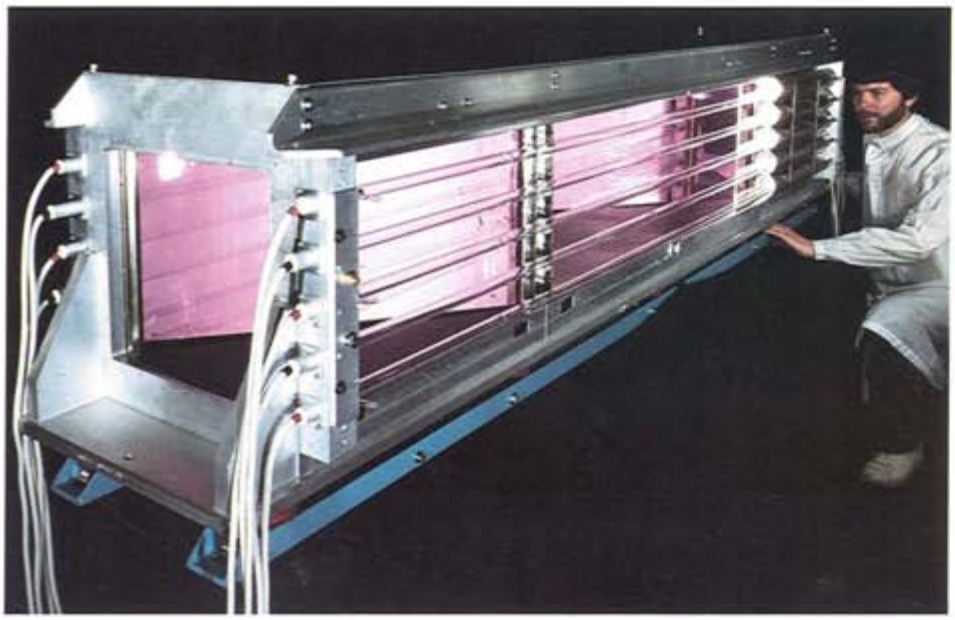

Figure 6. A single-segment amplifier prototype built to study features of Beamlet-type amplifier design. The horizontal tubes are the flashlamps, which are powered through the electrical cables attached to the device. The phosphate laser glass has a characteristic purple color. The design goals include improved efficiency and enhanced storage density.

Figure 7. A prototype close-coupled amplifier module with a 30- by 30-cm aperture for use in a multiple-segment amplifier. Half of the flashlamps are in the central array to improve efficiency. The protective clothing worn by the technician helps to prevent the equipment from being contaminated by dust particles that could cause damage during the passage of intense pulses of laser light. Note that corrugated white ceramic insulators are required to withstand the high voltages used in the flashtubes.

Although a Beamlet demonstration based on SSA-style hardware would be less expensive than one based on MSA-style hardware, it would not address many issues of segmented amplifier design and performance. Because we have never used a segmented amplifier of this sort in an operating system, we have decided to use MSA-style hardware for the Beamlet demonstration to clearly demonstrate segmented-aperture performance. As stated above, we will study the laser performance of only one of the four beamlets. To minimize cost, we will use lower-quality glass slabs in the three inactive beamlets.

Optical Damage

The fluence and intensity in the Beamlet demonstration will be limited by laser-induced damage to the optical components in the system. We have worked for many years to understand the mechanisms of damage and to raise the optical damage threshold of laser components. Our experience shows that the optical damage of interest under Beamlet conditions is caused by laser heating of microscopic absorbing inclusions and defects in the bulk of the optical materials, on surfaces, or in thin coating films. To achieve a high damage threshold, we must minimize the size and concentration of these defects.

We have also shown that the damage threshold of some defects can be raised by a "laser-conditioning" of the optical materials in which the laser fluence is slowly raised over a number of pulses.[6] Experiments with Nova have shown that the conditioning effect holds for large optics and is permanent. Because conditioning can raise the damage threshold by a factor of two or more, it can be quite important for high-fluence laser designs.

Table 1 summarizes the current status of laser damage thresholds for material and coating samples that we plan to use in the high-fluence regions of the Beamlet. The thresholds vary somewhat about the mean, so the safe working fluence of a coating with a statistical variation in defects lies below the mean threshold. We have chosen a safe working fluence of 85% of the mean, which is consistent with the distribution we see in high-quality test samples. For laser-conditioned samples, we apply a further safety factor of 85%. This accounts for variations in the effectiveness of the conditioning, which depends on the rate at which the fluence is raised over a small number of shots.

Table 1 shows that a 1053-nm average fluence of 12 J/cm^2 at 3 ns, at the output of the laser, is a reasonable design point for the Beamlet demonstration. We expect the peak-to-average intensity modulation on the beam to lie between about 1.5:1 and 2:1, based on models and on Nova experience. Thus, the peak fluence in the beam at 1053 nm will be between 18 and 24 J/cm^2. With a 1.5:1 modulation, all components will be safe with the possible exception of the thin-film polarizer were it to see the full output fluence. This argues for the configuration in which the polarizer does not see that full fluence (see Figure 3). Mirrors will be at some risk if the beam modulation on them is above about 1.5:1. Thus, if they see the full output fluence, they should be placed after the output image relay or spatial filter since filtering reduces the beam peak intensity.

We expect to see about 70% frequency-conversion efficiency and 90% beam-transport efficiency in the output from the Beamlet, so the 351-nm optical components will be subject to average fluences of 7.6 to 8 J/cm^2 at 3 ns. We expect a safe working fluence of about 11 J/cm^2 as shown in Table 1. These optical components should be safe,[7] provided that the beam modulation at 351 nm remains below about 1.4:1. With current optical technology, these components will be at the highest risk for damage as we raise the average fluence of the Beamlet in the configuration shown in Figure 3.

Amplifier Performance

For more than 20 years the LLNL laser program has devoted considerable effort to understanding the performance of glass lasers. We have studied analytical and empirical models of amplifier performance, flashlamp pumping, cavity transfer efficiency from flashlamp to glass, losses in a slab or disk caused by amplified spontaneous emission (ASE) trapped within the slab by total internal reflection, the effect of absorbing-edge claddings on those losses, and many other features of amplifier design. These models have been tested by comparing them to experimental data on the SSA and MSA prototypes, the Nova amplifiers, and other test systems. We use these data to project the performance of the amplifiers for the Beamlet.

Table 1. **Current status of laser damage thresholds of optical components.**

Component type	Damage threshold, J/cm^2 with pulselength (τ) in ns	Safe peak working fluence, J/cm^2 at 3 ns with safety factor*
1053-nm high reflectivity mirror†	$19\tau^{0.3}$	18
Thin-film polarizer†	$14\tau^{0.3}$	14
Bulk KDP‡	$20\tau^{0.5}$	24
Surface§	$22\tau^{0.4}$	29
351-nm bulk KDP	$9\tau^{0.5}$	11
351-nm surface§	$10\tau^{0.4}$	13

*The safety factor is 0.85 for damage threshold variation and for variation in the effectiveness of conditioning for laser-conditioned components.
†The high reflectivity mirror and polarizer are electron-beam-deposited, laser-conditioned HfO_2-SiO_2 multilayer stacks.
‡"Bulk" applies to high-damage-threshold KDP and KD*P (laser-conditioned). High-quality synthetic fused silica glass has significantly higher bulk threshold.
§"Surface" refers to optically polished surfaces on KDP or to fused silica that is either bare or coated with silica sol-gel.

There are two important design parameters for describing the laser performance per unit beam area of a glass laser amplifier using Brewster's-angle slabs or disks. These are the average gain per unit length averaged throughout the slab and the gain per slab as seen by the laser beam. The average gain per unit length is proportional to the average stored energy density, which determines the ratio of the growth in energy to the growth in nonlinear phase shift as a high-intensity pulse propagates through the amplifier.

The gain per slab g (in nepers) is proportional to the energy stored per unit area and determines the number of slabs we must have in series to reach the desired output fluence from the amplifier. As a rough estimate, with typical losses and tolerances on pulse distortion, we can expect to extract a net output in long pulses of up to about 70% of the stored energy in the area filled by the output beam. Shorter pulses will be limited to lower extracted fluence by nonlinear phase shift and optical damage.

Figures 8 and 9 show projections from the amplifier model for how the average stored energy density or gain coefficient a and the gain per slab g vary for a glass amplifier as a function of aperture area and thickness. The projections assume values similar to those used in the SSA and MSA prototypes for parameters such as the packing density of flashlamps, the flashlamp pulse length, and the cavity transfer efficiency. We assume that the energy delivered to the flashlamps is 20% of the energy at which a flashlamp explodes on a single shot in free air ($f_x = 0.2$), which is typical of Nova operating conditions. We also assume that the amplifier aperture is square, though the projections are not highly sensitive to aperture shape at constant area over the parameter range shown in the figures. Note also that, since the slabs are at Brewster's angle to the beam, the slab area is significantly larger than the aperture area perpendicular to the beam path in air. It is this latter area that we will discuss here.

Consider first the effect of slab thickness. Thin slabs have a higher energy storage density and can add more energy to the beam for a given increment in nonlinear phase shift, but they absorb light inefficiently. These slabs give better performance under short-pulse conditions, where the nonlinear phase shift is most important. On the other hand, thicker slabs absorb well and, with their lower average gain, have less stored energy loss from ASE; thus, fewer slabs are needed to reach the desired value of energy stored per unit beam area, and the energy storage bank is smaller. The design of a glass amplifier always involves a trade-off between many thin slabs with lower nonlinear phase shift and better short-pulse performance, and fewer thick slabs that store energy more efficiently and at a lower cost at a fixed aperture area. Most glass lasers at LLNL and elsewhere have been

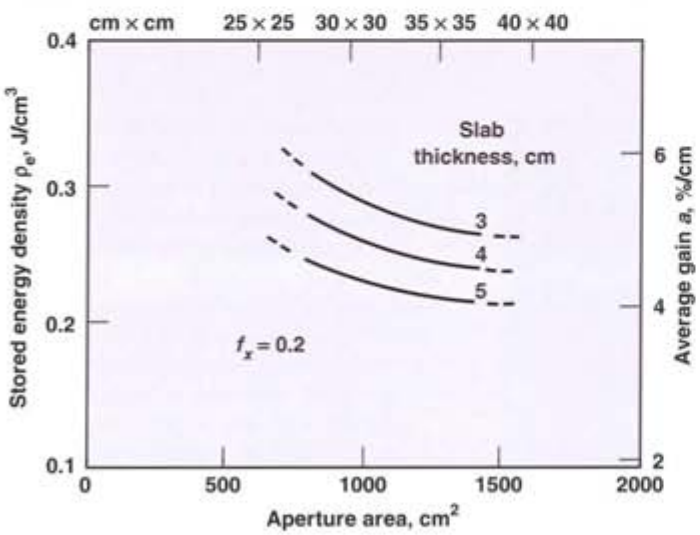

Figure 8. Energy storage density predicted by the LLNL amplifier model as a function of aperture area and slab thickness. Higher storage density means superior laser performance for short pulses. The energy storage density decreases for larger and thicker slabs but depends only slightly on area.

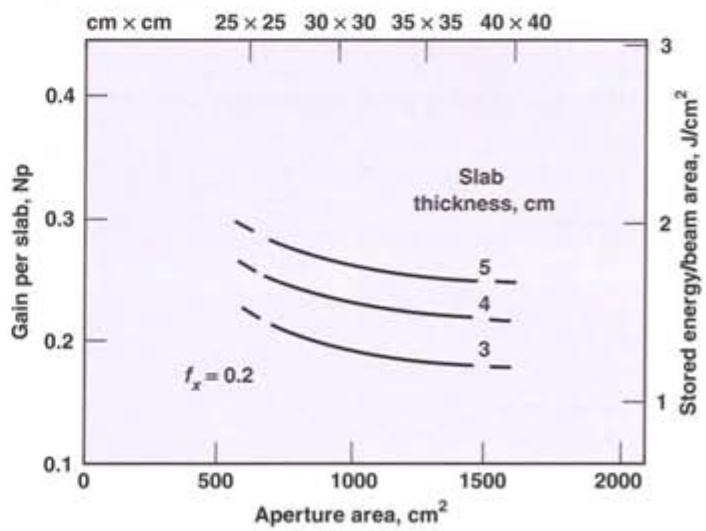

Figure 9. Gain per slab predicted by the LLNL amplifier model as a function of aperture area and slab thickness. Higher gain means that fewer amplifier slabs are required. The gain decreases for larger and thinner slabs, but change in gain with slab area is relatively slight.

built with a slab thickness of about 4 cm for large slabs, and we plan to use slabs near 4 cm in thickness for the Beamlet.

Figures 8 and 9 show that amplifiers of larger area have greater losses from ASE because they have longer gain paths before encountering the absorbing edge cladding and therefore store less energy for given pumping conditions than smaller amplifiers. The stored energy density degrades rather slowly with increasing area, however. This suggests that Beamlet areas larger than 900 cm^2 may not significantly affect performance. A significant fraction of the cost of a Beamlet does not scale with aperture, and there are no obvious reasons why the cost per unit area of optical components should jump abruptly over the region of interest. Therefore, because a larger Beamlet aperture would reduce the cost of an ignition facility, these operating conditions will be explored.

The open ends of a Brewster's-angle-slab amplifier lead to a gain gradient across the last slab near the end since one side of the slab sees less flashlamp light than the other. Tests on the MSA and SSA prototypes and on Nova amplifiers show that this gradient is roughly linear. If there is an odd number of slabs in each amplifier, the linear gain gradients at the two ends cancel and the gain is uniform across the aperture. By maintaining gain uniformity, we can keep the intensity profile uniform across the aperture. Therefore, we require an odd number of slabs for all Beamlet amplifiers.

Laser Performance

We use a number of different analytic and numerical models to predict laser performance. Figure 10 shows results from a laser performance code we use to evaluate the limits to output fluence set by nonlinear phase shift for the beamlet design shown in Figure 3. Based on Nova and other experience, we suppose that we must stay below a nonlinear phase shift of 2 rad between any two spatial filter pinholes in the system at the end of a square output pulse. There are two paths over which the phase shift is important for these conditions: the last double-pass through the inner amplifier (between spatial filter pinholes of the intracavity spatial filter) and the final passage through the switch and booster amplifier to the output spatial filter. For long pulses, the phase shift is larger in the inner amplifier; for short pulses the limit shifts over to the switch and booster.

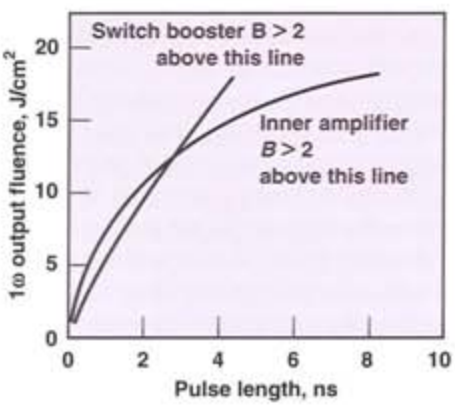

Figure 10. Projected Beamlet output fluence as a function of pulse length. Data are for a fixed 2-rad, nonlinear phase shift at the end of a square output pulse. The amplifier has 4-cm-thick slabs with an aperture area of 1100 cm^2 (see Table 2). There are 11 slabs in the inner amplifier and 5 slabs in the booster amplifier. For long pulses, the output is limited by the phase shift in the inner amplifier; for short pulses the limit shifts over to the switch plus booster. We have selected the number of slabs in each amplifier to place this transition at about 2 ns to optimize performance at 2 to 3 ns.

Table 2. Parameters assumed in performance simulations.

Reflectivity or transmissivity		
Amplifier slab (passive)		0.99
Mirror		0.99
Spatial filter		0.98
Switch (through polarizer)		0.92
Switch (reflection from polarizer)		0.94
Gain per slab	$f_x = 0.2$	
Thickness, cm	**Amperture area, cm^2**	**Gain, Np**
3	1400	0.18
	1100	0.19
4	1400	0.22
	1100	0.23
5	1400	0.25
	1100	0.26
6	950	0.29

For $f_x = 0.3$, multiply gain by 1.18.

Thickness (fused silica equivalent) for nonlinear phase shift, cm	
Lens	4
Pockels cell	7

The total number of slabs in the Beamlet is determined by the energy that must be stored to reach the desired output fluence, but in the two-amplifier configuration, we can shift slabs between the inner amplifier and booster to change the crossover point for the nonlinear phase shift in Figure 10. We have adjusted the split to put the crossover at about 2 to 3 ns since that maximizes the fluence that we can extract in 2- to 3-ns pulses; we expect this to be the most important operating range for the Nova Upgrade. The model also evaluates the required input fluence and pulse shape to reach a square output pulse at a particular fluence. For example, a 900-cm^2 output beam in an 1100-cm^2 amplifier at 12 J/cm^2 will require an input energy of slightly more than a joule, and the input pulse will have an intensity ratio from the leading edge to the trailing end (a "square pulse distortion") of about 8. The input pulse shape compensates for saturation in the Beamlet so that the output pulse is square.

Figure 11 compares a number of different Beamlet amplifier design options that are laid out in the same inner amplifier/booster amplifier configuration of Figure 3 but have different amplifier areas, slab thicknesses, and flashlamp explosion fractions. The design parameters are listed in Table 2. The reference operating point is 12 J/cm^2 at 3 ns. Figure 11 shows that we can readjust the number and position of slabs in the two amplifiers so that the nonlinear phase shift is roughly 2 rad at this point for a rather wide range of slab thicknesses, beam areas, and flashlamp explosion fractions. These parameters, then, are not particularly critical in reaching this operating point for the Beamlet if we choose the proper distribution of slabs between the two amplifiers.

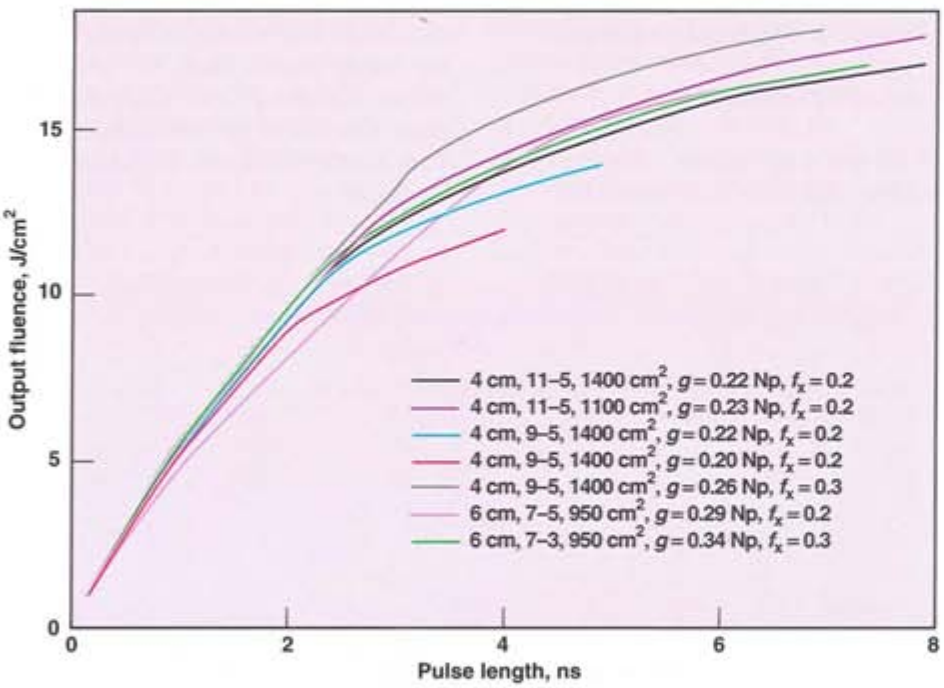

Figure 11. Comparison of a number of Beamlet designs optimized for operation at 2 to 3 ns. We can choose the number and placement of slabs to meet the design requirement at 2 to 3 ns over a large range of slab thicknesses, areas, and pumping conditions. Thick slabs pumped weakly will have significantly lower output at shorter pulse lengths, and configurations having low stored energy per unit area will have significantly lower output at long pulse lengths. Configurations having many thin, highly pumped slabs can reach higher fluence at constant nonlinear phase shift, but we would not choose these costly configurations unless damage thresholds were to improve to the point where we could run the system at these higher fluences.

The performance at other operating points will vary somewhat. We see from Figure 11 that thick slabs pumped weakly, for example, will have a significantly lower fluence limit for short pulses and that amplifiers storing less energy per square centimeter of aperture will not be able to reach as high a fluence for long pulses. Large numbers of thin, highly pumped slabs could permit higher fluences at 2 rad of phase shift, but damage thresholds of current components prevent us from operating there. We expect to use 16 slabs in the Beamlet for the initial series of experiments since this is where we think we can optimize the performance/cost ratio for typical ignition-target irradiation pulses; but we will also be able to test other configurations to check our models.

The Focal Plane

There are a number of important components near the focal plane of the intracavity spatial filter, such as:

1. Optics to inject the input pulse to the Beamlet.

2. The spatial filter pinhole array.
3. A beam trap to intercept laser energy that is not switched out of the cavity by the Pockels cell.
4. Provisions to prevent pinhole debris from contaminating the optics.
5. Absorbing surfaces to deal with stray back-reflected beams and to prevent parasitic oscillations from glints near the focal plane.
6. Laser alignment components.

We discuss items 1–3 briefly in this article. The present concepts for items 4–6 appear schematically in several figures but will not be discussed in detail.

The most challenging component in the focal plane is the beam trap, which must be small and able to survive under adverse conditions. The size of the beam trap is important because it dictates the size of the off-axis angle in the multipass cavity. Since a large off-axis angle—and therefore a large beam trap—causes us to use the aperture of the inner amplifier less efficiently, a small off-axis angle—and therefore a small beam trap—is highly desirable. The Pockels cell will switch about 6 to 8 kJ on a normal Beamlet shot. Since 1 to 3% of the energy in the cavity may leak through the switch, the beam trap should be capable of surviving up to about 200 J on every shot without serious degradation or harmful back-reflections into the laser.

The beam-trap design that we plan to use is shown in Figure 12. The trap is split into two sections upstream and downstream of the focal plane. Since the beam inverts in passing through the focal plane, this split allows us to intercept the beam at twice the distance from the focal plane (or four times the area) that we would be forced to use if we intercepted the beam where it is fully separated from the adjacent, earlier pass through the cavity. The beam strikes a primary absorbing glass surface at each of the two trap positions; any light reflected from those surfaces strikes secondary absorbing glass surfaces well out of the beam path. The trap before the focus has a surface configured to spread the reflected beam so that it does not come to a focus near the secondary absorber.

If we separate the pinholes in the focal plane by 3 cm, then the primary absorber intercepts the beam at about 150 cm from focus, where the area of the beam is 36 cm^2. The area of the absorber is somewhat larger since it is at an angle to the beam. We have tested a one-eighth scale model of the beam trap under conditions corresponding to normal operation and switch failure, and it performed adequately.

Figure 13 shows the multiple-pass pinhole layout that we expect to use for the first series of Beamlet experiments, shown as it would appear from the switch side of the spatial filter (looking toward the pinhole array with the inner amplifier and mirror M1 beyond it). The input pulse is injected through pinhole 1 in the figure. The exact retroreflection point R1 of mirror M1 is in the center of the array of pinholes 1, 2, 3, and 4, so the return pulse goes through pinhole P2 after a double-pass through the inner amplifier with a reflection from M1. It then goes through the switch and is reflected from M2, which has a retroreflection point, R2, midway between pinholes

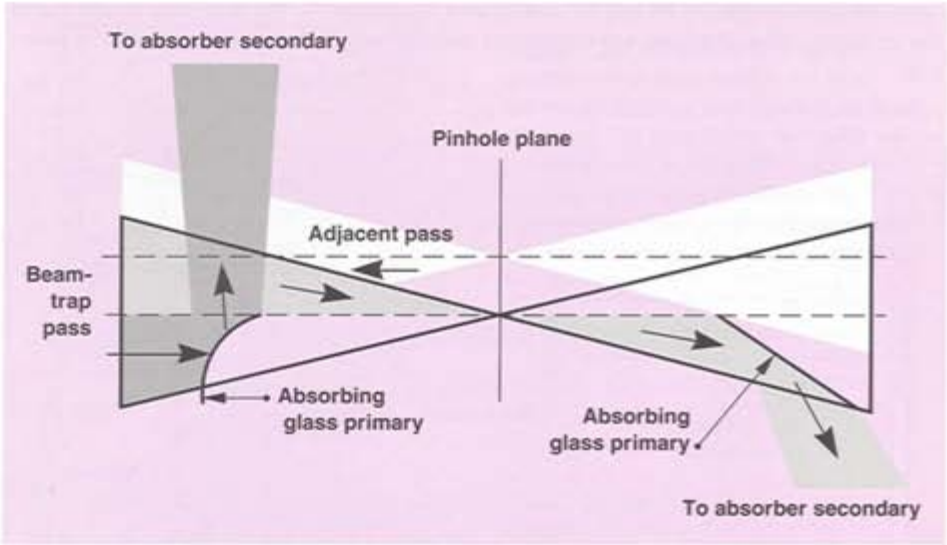

Figure 12. Design of the beam trap in the intracavity image relay. The beam trap intercepts any laser energy that is not switched out of the multipass cavity when the Pockel cell switch fires. There are two primary traps made of absorbing glass—one located upstream and the other located downstream of the focal plane. Using two traps allows us to have four times the absorbing area at a fixed separation from the adjacent beam in the focal plane. The energy reflected from the primary traps is absorbed by secondary traps well out of the beam path.

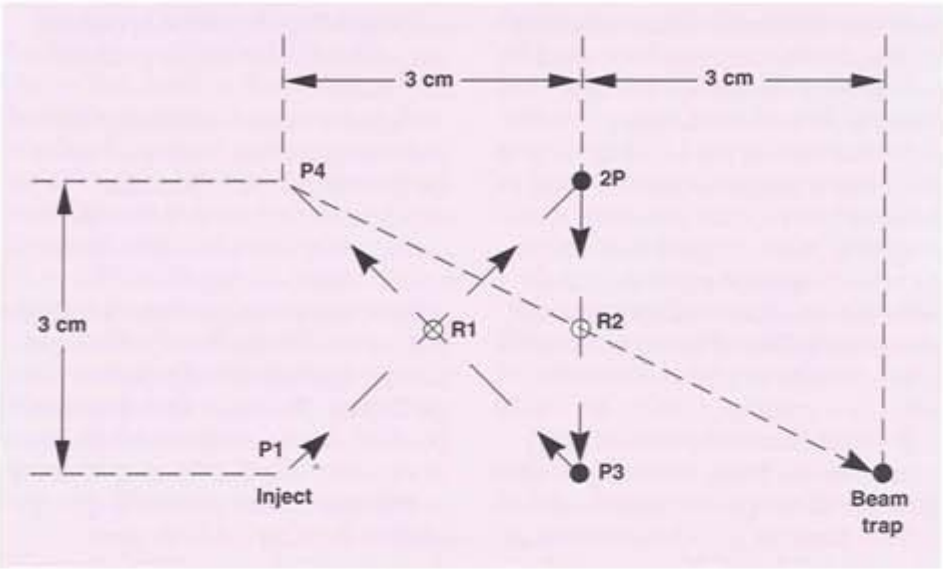

Figure 13. Beam spatial filter ("pinhole") array in the focal plane of the intracavity image relay, looking from the switch side of the array towards the inner amplifier and mirror M1. The beam enters through pinhole P1, going into the plane of the array and figure towards M1. The retroreflection point of M1 is R1 in the center of the square array of pinholes P1, P2, P3, and P4. Thus, the return beam from M1 comes out of the figure through pinhole P2. It then goes through the switch and reflects from mirror M2, which has a retroreflection point R2 centered between pinhole P2 and P3, and returns to pinhole P3. The final pass comes out of the array through pinhole P4. Any energy not switched out of the cavity returns to the beam trap.

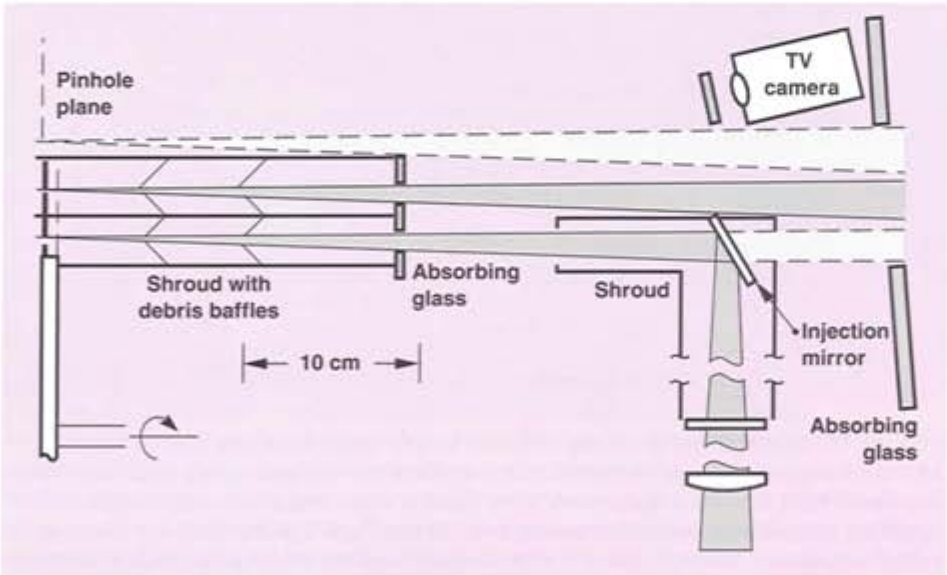

Figure 14. Top view of the center of the spatial filter, located in the relay focal plane. This view shows the layout of injection optics in this region. The absorbing glass removes unwanted energy from the system. Debris baffles trap any hot particles produced by pinhole damage and thus prevent contamination of the optics. The TV camera is part of the diagnostics system.

P2 and P3, and the return pulse from M2 goes through pinhole P3. The pulse then makes a final double pass through the inner amplifier and emerges through pinhole P4. Meanwhile, the switch has been fired so that the pulse is switched out at the polarizer. Any switch leakage returns to the pinhole plane at the position marked "beam trap." This is the radiation that the beam trap must intercept.

Figure 14 is a top view of the center of the spatial filter showing the layout of the pinholes and injection optics. The input pulse enters the spatial filter through a window and reflects from an injection mirror located about 40 cm from the focal plane that contains the pinhole array. An injection lens focuses the input pulse on pinhole P1. The other components in the figure are absorbing surfaces, laser alignment components, and features to control pinhole debris.

Frequency Conversion

We convert the 1053-nm laser output beam to its third harmonic at 351 nm using nonlinear optical interactions in two sequential thin plates of KDP. The frequency converter for the Beamlet will have an input fluence and intensity of 12 J/cm^2 and 4 GW/cm^2 at the reference design point, which is a factor of three or four higher fluence and a somewhat higher intensity than typical operating conditions for Nova. We have achieved[8] a conversion efficiency of up to 80% on single Nova crystals at up to about 3 GW/cm^2, as shown in Figure 15. Because conversion efficiency depends upon instantaneous intensity rather than integrated fluence, these values should be achievable at the same intensity on the Beamlet, although we may wish to optimize

the converter design for a somewhat higher intensity than was used in the Nova design. There are few data at high fluence because crystals that can withstand high fluences have become available only recently.

Figure 16 shows the expected performance of two candidate converter designs for the Beamlet, recalculated from the Nova design for a slightly higher working intensity. We use the code developed for analyzing the performance of Nova frequency converters to study these design changes. These plots assume that the detuning angles and intensity profiles on the beam are similar to those we use to fit the data from Nova. The model indicates that we should be able to operate frequency converters above 70% efficiency, over a range of about a factor of three in intensity near the nominal Beamlet operating point. Frequency conversion tests to validate this performance will begin soon on a small (~100-J) laser at LLNL.

Stimulated Scattering Losses

The Beamlet runs at intensity, fluence, and beam aperture large enough for transverse stimulated scattering to occur in optical components. The thresholds are lowest in the components that see the third harmonic—i.e., the frequency converter and any optical components that follow it. These processes can lead to a significant energy loss from the beam and must be considered in the design.

We have studied transverse stimulated Brillouin scattering (TSBS) in fused silica[8] with the Nova laser, which can reach conditions up to about 2.5 times the threshold at which TSBS becomes important. Our experiments demonstrate that TSBS can be suppressed by imposing a rather small frequency bandwidth on the laser. SRI International has measured SBS gains in KDP and other optical materials for us, and these measurements show that the gain in KDP is comparable to that in fused silica.

The reference operating point for the Beamlet is about 5 to 6 times the TSBS threshold, and SBS models suggest that we will need a bandwidth at 351 nm of about 50 to 90 GHz to suppress TSBS under these conditions.[8] The bandwidth required to suppress TSBS in the Nova experiments was somewhat less than that predicted by the models. Frequency conversion efficiency can be reduced at large bandwidth, but our models predict that bandwidths of this magnitude are too small to have a significant effect on efficiency.

The Beamlet also runs close to the threshold for transverse stimulated Raman scattering (TSRS) in the KDP frequency conversion crystals at 351 nm. The transverse Raman gain in KDP was studied[9] during the design of the Nova frequency converters, and is about 0.23 cm/GW in the direction of highest gain at 351 nm in a tripler. The 351-nm intensity near the output face of the Beamlet tripler is about 2.7 GW/cm^2 for the reference operating point, so the transverse Raman gain is roughly e^{20} for a single transit across the crystal aperture—a high enough gain that TSRS may go over threshold. It is clear that the edges of the KDP crystals must be designed to prevent multiple reflections across the crystals.

One option for the frequency converter reduces the TSRS gain by a factor of about 2.6 and eliminates

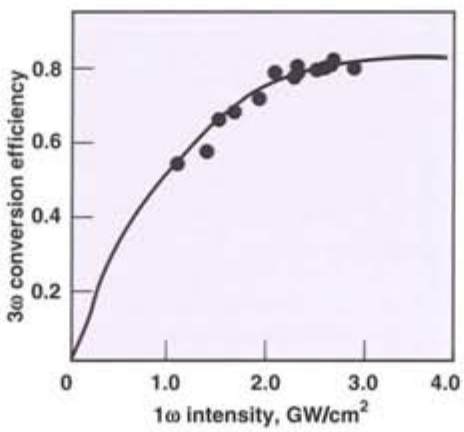

Figure 15. Efficiency of frequency conversion of laser light to the third harmonic (350 nm) as a function of input intensity. The data points represent values measured with a set of KDP frequency conversion crystals used on Nova. The conversion efficiency is as high as 80%. We expect to achieve similar values with the Beamlet.

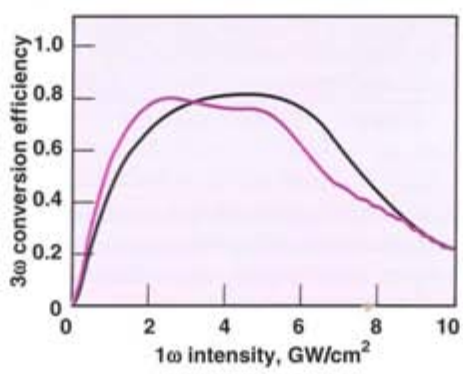

Figure 16. Frequency conversion efficiency as a function of input power for two candidate converter designs for the Beamlet experiments. We calculated beam intensity profiles, divergence, and angular misalignment using Nova parameters. The black line is a type I-II converter with 1.05- and 0.8-cm crystal thicknesses. The colored line is a similar converter but with 1.2- and 1.05-cm-thick crystals.

TSRS as an issue. Figure 17 shows the spectra of transverse Raman scattering in KDP and KD*P viewed in the direction having highest TSRS gain in the orientation used in a tripler. The sharp peak of highest gain at about 920 cm^{-1} is the symmetric stretch vibration of the phosphate PO_4 tetrahedron in the crystal. In the deuterated crystal, this peak splits into two features having much lower amplitude. We plan to have deuterated as well as undeuterated frequency converter crystals available for use on the Beamlet.

Edge Effects and Allowances

The useful part of a laser beam is the flat-top region of uniform intensity in the center, but there are a number of edge effects around the perimeter that can force the beam and components to have a somewhat larger area. In this section, we discuss the most important of these effects and the allowances for them in the Beamlet design.

Apodization

If the intensity drops abruptly to zero at the edge of the beam, a diffraction ripple will grow into the beam as it propagates and will develop a peak intensity of 1.4 times the mean intensity of the beam. The interaction of the two sides at a square corner raises the intensity to twice the mean. We wish to keep a uniform intensity profile and must suppress this ripple growth.

The standard technique to suppress edge diffraction of this sort is known as apodization. The edge of the beam must have an intensity profile that "rolls off" smoothly to zero over a distance of at least several Fresnel zones, as seen over the longest unrelayed propagation distance over which the uniform intensity must be preserved.

Analysis with diffraction propagation codes suggests that a profile rolling off about 0.6 cm at each edge, with a rounded corner on the square aperture having a radius of 1.75 cm, will allow us to keep a uniform intensity over 90% of the area of a beam that has a zero-intensity aperture of 30 cm.

Edge Distortion Allowance

The amplifier slabs have an edge cladding around the perimeter to absorb the amplified spontaneous emission that is trapped within the slab by total internal reflection. This cladding is attached to the slab using an index-matched epoxy adhesive. The temperature of the cladding rises significantly as the disks are being pumped because it may absorb as much as 10 to 20 J/cm^2 of ASE radiation. The cladding then expands, distorting the slab and deviating optical rays near the edge of the slab. The distortion will probably be sufficient to affect beam quality in the laser for a distance of half the slab thickness from the edge. Thus, the amplifier slabs should be larger than the desired clear aperture by a margin of this size. To keep the cost down, optical components must also have an edge allowance for finishing operations; the thermal edge distortion allowance defined here should be adequate for that function as well.

Vignetting Allowance

The beam propagates through different pinholes on each pass through the cavity spatial filter, so its footprint on optical components changes slightly with each pass. Some components must be a little larger than the beam to allow for this beam motion.

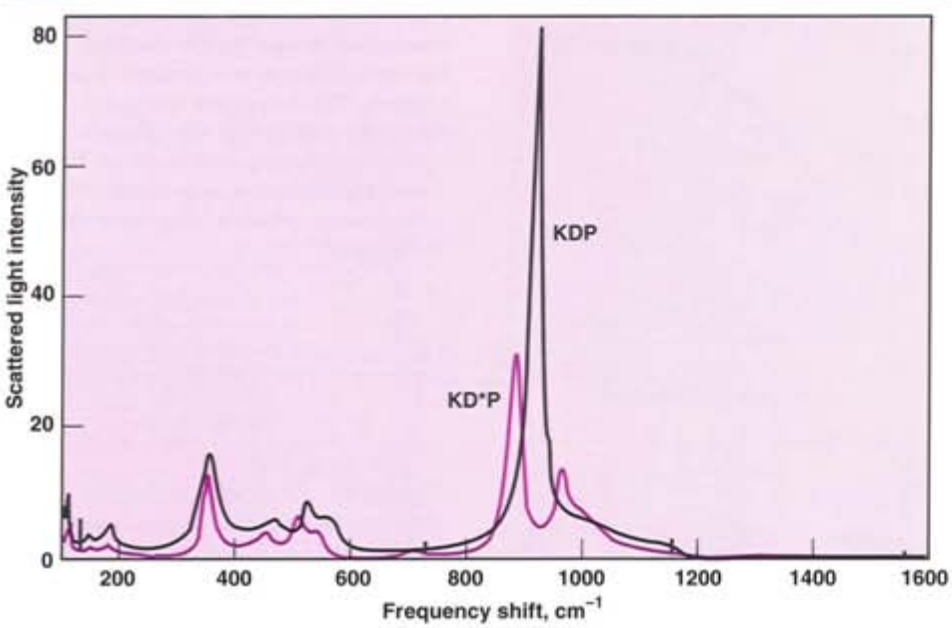

Figure 17. Spontaneous Raman scattering intensity of KDP and KD*P crystals measured transverse to the beam in a type II tripler. Scattered light represents a power loss. In the deuterated crystal KD*P, the phosphate peak at 920 cm^{-1} splits into two much smaller peaks, making the Raman gain (which is proportional to the spontaneous scattering intensity) much lower. We plan to have deuterated and undeuterated crystals available for use on the Beamlet.

Beam Aperture

The most cost-effective beam aperture is probably somewhat larger than our nominal aperture size of 30 cm. It is important that we address the issue of larger apertures in the Beamlet project in order to have data to make performance/cost analyses for an ignition facility. At the same time, there is a limit to the size of the KDP and KD*P crystals that we can acquire in time for the Beamlet activation in 1993. Growing these large crystals can take as long as two years. Discussions with vendors show that we can easily acquire crystals that will permit a 30-cm clear aperture for the switch and frequency converters in adequate time and that we can probably have crystals available in mid- to late 1993 for a beam clear aperture of 35 cm. (This requires a raw crystal of about 46 by 46 by 25 cm for cutting a type I frequency converter). Therefore, our first series of experiments will be conducted with a beam hard aperture of 30 cm, but we will design optics that permit an aperture of 35 cm when crystals for that aperture become available.

Cavity

The cavity must be long enough to accommodate the maximum number of amplifier slabs that can be used in Beamlet demonstrations. We have chosen a length of 36 m, which is longer than the minimum of ~30 m but gives more flexibility for alternative configurations and larger numbers of slabs. The spatial filter lens focal length is 9 m.

A very important feature of optical design for high-energy lasers is the placement of components to avoid the so-called "ghost foci" of the optical train. These are points at which stray reflections from lenses and other components come to an intense focus. We have tracked the paths of the ghost beams in the Beamlet layout and have found that all the foci fall within 3 m of the face of the spatial filter lenses for the lens design we plan to use. Thus to avoid this problem we must ensure that optical components are no closer than 3 m to the lenses.

Some of the ghost foci will reach intensities sufficient to cause air breakdown and generate small spots of plasma in the air within the laser. This is not an issue for the high-energy final passage through the cavity since any breakdown will occur after the laser pulse has gone through the volume in which the breakdown occurs. If there is air breakdown on early passes through the cavity, the effect on the beam will be much the same as if there were a small obscuration on an optical surface, such as a damage spot. There is not enough time between passes for the plasma to expand or for acoustic disturbances to propagate out from the breakdown volume.

Amplifier Slab and Spatial Filter Lens

We will purchase amplifier slabs large enough for an edge distortion that is about half the 4-cm thickness at the large (35 cm) Beamlet aperture option and the full slab thickness at the small (30 cm) option. The last slab of the inner amplifier on the spatial filter side requires the largest vignetting allowance of any amplifier slab, and we must size the amplifier clear aperture so that it will accommodate a 35-cm beam. If that amplifier is 11 slabs long, the aperture required for the last slab will be 38 cm. This gives an amplifier slab size, before final polishing and edge cladding, of about 77 by 43 by 4.4 cm. This slab has a volume of 14.4 liters and is about twice the size of the largest slabs poured for Nova. We have placed an order for these slabs, and they will be poured this year.

The largest component in the Beamlet configuration shown in Figure 3 is the spatial filter lens on the inner amplifier side of the intracavity spatial filter since that lens has the largest vignetting allowance in the system. We plan to have a clear aperture of 55 cm (diagonal) at that point.

Summary

We are developing a new modular laser architecture to increase the power and reduce the cost of lasers used for inertial confinement fusion experiments. The laser will be an assembly of optically independent units or modules called "beamlets." Each beamlet will have an aperture of about 30 cm and will deliver to the ignition target an output of 3.5 to 7.0 kJ at 351 nm. A 16-beamlet array would have nearly twice the energy output of the Nova laser.

We have ordered long lead-time optical materials (KDP crystals, laser glass, and fused silica) and are now proceeding to the detailed design and testing of prototypes for the major components. We expect to have the full system operational in late 1993. We shall then test a number of modifications to the basic design to optimize the Beamlet design for an ignition facility.

We expect that this modular laser architecture, with its associated economies of scale and procurement, will demonstrate the improved, cost-effective technology and performance required to meet the goals of the national Inertial Confinement Fusion Program.

Key Words: beamlet; fusion target; high-power lasers; laser architecture; inertial confinement fusion (ICF); Nova laser.

References

1. J. T. Hunt and D. R. Speck, "Present and Future Performance of the Nova Laser System," *Opt. Eng.* **28**, 461–468 (1989); W. W. Simmons and R. O. Godwin, "Nova Laser Fusion Facility—Design, Engineering, and Assembly Overview," *Nucl. Technol./Fusion* **4**, 8–24 (1983).
2. National Research Council, National Academy of Sciences, *Second Review of the Department of Energy's Inertial Confinement Fusion Program, Final Report* (National Academy Press, Washington, D.C., (1990).
3. *Fusion Policy Advisory Committee, Final Report*, U.S. Department of Energy, Washington, D.C. (1990).
4. Secretary J. D. Watkins, letter to Hon. R. S. Walker, ranking minority member, Committee on Science, Space, and Technology, U.S. House of Representatives, Washington, D.C., 21 February 1991.
5. W. W. Simmons, J. T. Hunt, and W. E. Warren, "Light Propagation Through Large Laser Systems," *IEEE J. Quantum Electron.* **QE-17**, 1727 (1981).
6. J. H. Campbell et al., "Damage-Resistant Optics for a Megajoule Solid-State Laser," *SPIE Proceedings* **1441**, 444–456 (1991); *Laser-Induced Damage in Optical Materials: 1990*, LLNL Preprint, UCRL-JC-1004900 (1990).
7. K. E. Montgomery and F. P. Milanovich, "High-Laser-Damage-Threshold Potassium Dihydrogen Phosphate Crystals," *J. Appl. Phys.* **68**, 3979–3982 (1990).
8. J. R. Murray et al., "Experimental Observation and Suppression of Transverse Stimulated Brillouin Scattering in Large Optical Components," *J. Opt. Soc. Amer. B* **6**, 2402–2411 (1989).
9. W. L. Smith, M. A. Henesian, and F. P. Milanovich, "Spontaneous and Stimulated Raman Scattering in KDP and Index-Matching Fluids," *Laser Program Annual Report 1983*, LLNL Rept. UCRL-50021-83 (1983).

For further information contact
John R. Murray (510) 422-6152,
John H. Campbell (510) 422-6497,
D. Neil Frank (510) 422-1742,
John T. Hunt (510) 422-5467,
or John B. Trenholme (510) 422-6228.